Probing the time-dependent decay of molecular core-excited states: The Auger resonant Raman effect for O_2

Zbigniew W. Gortel*
Department of Physics, University of Alberta, Edmonton, Alberta, Canada T6G 2J1

Dietrich Menzel†
Physik-Department E20, Technische Universität München, D-85747 Garching, Germany
(Received 20 April 1998)

We use our recently developed explicitly time-dependent theory for one-step resonant excitation-deexcitation processes of core-excited states in diatomic molecules to investigate the O $1s$ core-hole decay electron spectra of O_2. Looking at the changes of the spectra as the exciting radiation frequency is tuned to and away from the excitation resonance allows us to follow the time evolution of the nuclear degrees of freedom of the molecule in the short-living core-excited state. We explicitly demonstrate that here, in contrast to other diatomic molecules such as N_2 or CO investigated earlier, the relative softness of the intramolecular bond in the core-excited state allows us to interpret changes in some gross features of the decay spectra with varying photon energy in terms of the classical time evolution in the excited state. In particular, the low-energy tail of the electron spectra, due to the fraction of the core-excited state molecules surviving longest, gets visibly suppressed if the exciting radiation is detuned away from the x-ray-absorption resonance.
[S1050-2947(98)06211-8]

PACS number(s): 33.80.Eh, 34.10.+x, 34.50.Gb

When a core electron of an atom or a molecule is promoted by external radiation to an unoccupied orbital, the resulting core-excited state decays via emission of a photon or of an Auger electron within times which, for molecules, may be shorter than the oscillation period of the molecule in the core-excited state. With the advent of third-generation synchrotron radiation sources with high brightness combined with monochromators with high-resolving power, it is now possible to initiate the core-hole decay processes using a bandwidth of the exciting radiation which is narrower than the core-level lifetime width [1]. Under such conditions, termed the resonant x-ray Raman scattering conditions (for photon detection) or the radiationless resonant Raman scattering or Auger resonant Raman scattering (ARRE) conditions (for electron detection), the excitation-decay sequence has to be treated as a single process. The decay spectra then exhibit interesting features: tuning the narrow excitation line across and away from the excitation resonances leads to distinct qualitative changes of the spectra, including changes in the number and shapes of their peaks, as follows [1–4]: (i) The decay spectra energies as the incoming radiation is tuned across the excitation resonance(s) are generally expected to shift linearly (''linear dispersion''), because of energy conservation for the overall process: the decay products, electrons or photons, must accommodate the surplus energy of the incoming photons. The shift can, however, be in fact *nonlinear* for nonideally monochromatic radiation. (ii) Although the magnitude of the cross section follows the resonance profile (''resonance enhancement''), the linewidths of the decay spectra are not affected by the short lifetime of the core-excited state and are narrower than the lifetime width (with their widths limited by the final state lifetime), i.e., the lines are in fact narrower than the corresponding normal Auger lines (''line narrowing''). (iii) The decay spectra lines are often asymmetric and can even exhibit a double-peak structure (''Stokes doubling''). (iv) For molecules an additional factor influencing the appearance of the spectra is the presence of effects related to the lifetime-broadened vibrational structure of the core-excited state and of the vibrational structure of the molecule after decay (''lifetime-vibrational interference'') [5–8]. Electron or x-ray decay studies under nearly or truly resonant Raman conditions are now vigorously pursued for small diatomic molecules such as CO [6–11], adsorbed CO [12], N_2 [6,13], O_2 [6,14,15], HCl [16,17], and others.

Recently, we have developed an explicitly time-dependent theory for one-step resonant excitation-deexcitation processes of core-electron states in diatomic molecules [18] and have presented detailed discussions of the decay electron spectra obtained under ARRE conditions (subsequently abbreviated as ARRE spectra) for several decay modes of N_2 and CO. In particular, special attention has been paid to the influence which the time evolution in the core-excited state has on the appearance of the spectra. The explicitly time-dependent approach is particularly well suited for this purpose [19,20]. Apart from self-evident information about the vibrational structure of the final molecular ion, a great deal can be learned about the forces between the constituents of the molecule in the short-living core-excited state, when the time spans during which the decay spectrum is formed by the molecule evolving in the excited state can be externally controlled. This is possible under the ARRE excitation conditions, i.e., when the exciting x-ray radiation with a bandwidth below the lifetime widths of the excited state is swept across the absorption resonances and detuned away from them. In this paper we will apply the theory de-

*Electronic address: gortel@gortel.phys.ualberta.ca
†Electronic address: menzel@e20.physik.tu-muenchen.de

veloped in Ref. [18] to O $1s \rightarrow 1\pi_g$ excitation and its Auger decay to the lowest-energy final state in the O_2 molecule. We will gain insight into the time evolution of the system in the excited state by following the evolution of the spectra with varied tuning conditions of the exciting radiation. The results are complementary to those in Ref. [20], where similar insights were obtained by following the formation of the spectra in time. What distinguishes the O_2 molecule from N_2 and CO is the degree to which the internuclear forces get modified upon core-hole excitation: the relative increase in the equilibrium bond length and decrease of the oscillation frequency are very small in CO ($\sim 2\%$ and $\sim 4\%$, respectively), somewhat larger for N_2 ($\sim 6\%$ and $\sim 20\%$, respectively), but quite large for O_2 ($\sim 12\%$ and $\sim 31\%$, respectively). Consequently, the resonant excitation places O_2 higher on the repulsive side of the potential of the core-excited state than it does for the other two molecules. As we shall see in what follows, this permits us to understand qualitatively certain gross features of the O_2 ARRE spectra in terms of the classical time evolution of the system in the excited state. This does not imply, of course, that classical mechanics can be used to calculate the ARRE spectra with all their rich details.

The microscopic processes involved in ARRE are visualized in Fig. 1 for the O_2 molecule. The molecules in their electronic ground state $X\,^2\Sigma_g^-$, in which the internuclear potential is $V_g(r)$, are continuously pumped by the x-ray radiation, promoting the O $1s$ electron to the half-filled valence molecular orbital $1\pi_g$. In a quantum-mechanical picture of the process, the initial wave function (the ground-state wave function of V_g), which describes the relative motion of the nuclei, is placed on the core-excited state potential curve, $V_d(r)$, along which it then evolves according to the time-dependent Schrödinger equation. The excitation process continues while previously excited wave packets move away from their initial position and the packets promoted at different instants mutually interfere [20]. The core-excited state of the molecule is unstable against the autoionizing decay which results in a free electron being emitted, leaving behind a molecule in a final ionic configuration in which the intramolecular potential is $V_f(r)$ (shown here for the O_2^+ ground state, i.e., the result of the decay to the final state of lowest energy).

Although the above description might suggest that the entire process is a sequence of three independent events—excitation, evolution, and decay—it must, nevertheless, be treated as one coherent quantum-mechanical process in which an x-ray photon is absorbed and an electron is emitted. One of the consequences is that, while energy conservation for the overall process requires the exact partitioning of the energy of the absorbed photon into the kinetic energy of the released electron and the energy remaining within the molecule (shared between its electronic and vibrational degrees of freedom), no restriction is imposed on the energy of the photon which may initiate the process—apart from the fact that the electron yield is enhanced when the radiation is in resonance with transitions to particular vibrational states of the core-excited molecule (resonance enhancement).

The lifetime of the core-excited state, $\tau = 7.3 \times 10^{-15}$ s, is shorter than the time needed for one vibrational oscillation in

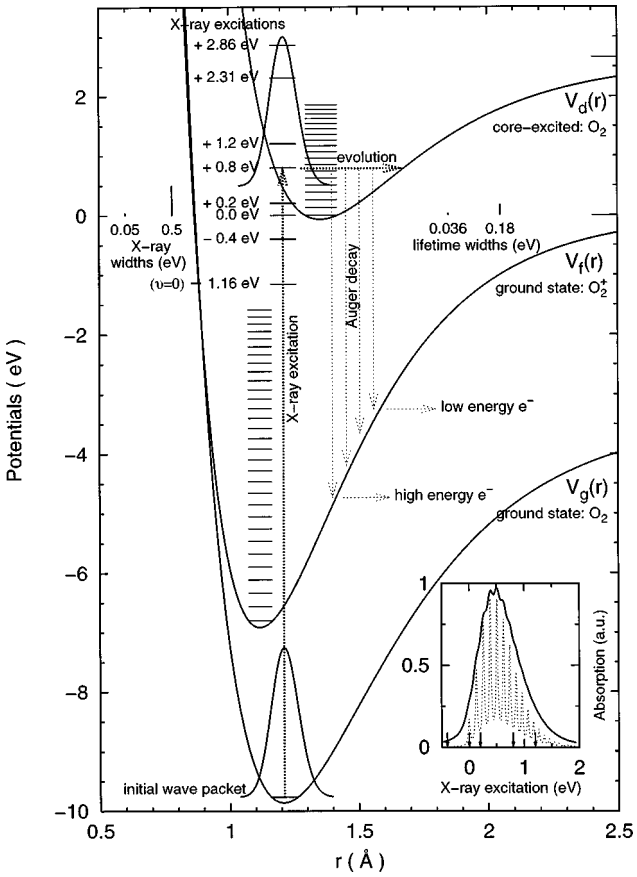

FIG. 1. Potentials used for the O_2 molecule (vertically displaced to fit the scale of the graph), vibrational levels for the core-excited and ionic state, and the initial wave packet. Eight x-ray excitations, used to calculate the spectra in the eight horizontal panels of Figs. 2 and 3, are represented by a dotted vertical arrow and horizontal bars labeled by the actual excitation energy (with respect to the resonant excitation energy to the $v=0$ vibrational level of V_d). X-ray bandwidths and lifetime widths (vertical bars), time evolution (horizontal dotted arrow), Auger decay (fine-dotted vertical arrows), and electron emission are also indicated. Inset: Calculated absorption spectrum for the actual core-hole lifetime (solid line) and for a hypothetical five times longer lifetime (dotted curve). Six out of eight x-ray excitations used are denoted by vertical arrows.

V_d (more than 3×10^{-14} s), which makes the lifetime width $\Gamma = 2\hbar/\tau = 0.18$ eV [6] comparable with the vibrational level spacing in this potential (cf. Fig. 1). Consequently, the straightforward x-ray-absorption spectrum is broad and structureless, enveloping over a dozen vibrational peaks that would only be separable if the lifetime were longer. This is seen in the inset in Fig. 1, in which the calculated absorption spectra (for ideally monochromatic radiation and ideal electron detector resolution) are shown for the actual and for a hypothetical lifetime, corresponding to $\Gamma = 0.036$ eV, five times longer than the actual one.

The dimensionless expression for the kinetic energy distribution of Auger electrons emitted by a diatomic molecule core-excited by x-ray radiation centered around the nominal frequency ω_L and decaying to the fth electronic configuration of an ion, as derived in Ref. [18], is

$$S(\mathcal{E}) = \omega_d^3 \sum_{n'} G[(E^f_{n'} + \mathcal{E} - E_{\rm in} - \hbar\omega_L)/\hbar] \times \left| \int_0^\infty dt\, e^{i/\hbar(E^f_{n'}+\mathcal{E})t} e^{-\Gamma t/2\hbar} \langle u^f_{n'} | u_d(t)\rangle \right|^2 . \quad (1)$$

Here, $\mathcal{E}$ is the electron kinetic energy, $G(\omega-\omega_L)$ is a Gaussian with a full width at half maximum (FWHM) (denoted Γ_L) accounting for the spectral distribution of the radiation, $E_{\rm in}$ is the initial energy of the system (ground-state energy of V_d), $u^f_{n'}(r)$ and $E^f_{n'}$ denote, respectively, the wave function and the energy of the n'th vibrational state of V_f, and $u_d(r,t)$ is the time-dependent wave packet evolving along the core-excited state potential V_d. The actual differential cross section is obtained by multiplying $S(\mathcal{E})$ by $\Gamma_f \omega_L D^2/2c\hbar^3\omega_d^3$, where D is the transition dipole moment of the initial excitation, ω_d is the frequency parameter of V_d, and Γ_f is the contribution to the total lifetime width Γ due to the Auger decay to the particular final electronic configuration f of the ion.

The time-dependent wave packet $u_d(r,t)$ is a linear combination of terms $\propto \exp(-iE^d_v t/\hbar)$ oscillating in time. Here, E^d_v are the energies of vibrational levels in the core-excited potential V_d. The largest contribution to the wave packet is due to several levels grouped around $v=4$, as seen in Fig. 1. Therefore, for nearly monochromatic radiation [i.e., narrow $G(\omega-\omega_L)$], the effective time interval during which the time evolution of the wave packet contributes to the formation of the spectra in the integrand of Eq. (1) is equal to $\tau_{\rm eff} = 2\hbar/\Gamma_{\rm eff}$ [21] with

$$\Gamma_{\rm eff}/2 = \sqrt{\Omega^2 + (\Gamma/2)^2}, \quad (2)$$

where in the present case $\Omega \approx \hbar\omega_L - E^d_{v=4}$ is the detuning of the radiation away from the most efficient resonant excitation. For resonant excitation the wave packets are promoted to the core-excited state potential at such instants at which their phase agrees with the phase of the time-evolved wave packets promoted earlier. They then interfere constructively and their residence time on the core-excited state surface is limited solely by the core-hole lifetime $\tau = 2\hbar/\Gamma$. No such phase correlation occurs for large detunings, which causes destructive interference between packets promoted at different instants, and the effective time of the spectra formation becomes considerably shorter than the core-hole lifetime.

The spectra are calculated from Eq. (1) using Morse potential representations for V_g and V_f resulting in analytic expressions for $u_d(r,t=0)$ and for $u^f_{n'}(r)$ [18]. The time evolution of the wave packets is followed by numerically solving the time-dependent Schrödinger equation. Any form of V_d can be used but in this work we choose the Morse form also for this potential. The parameters [6] used in the calculations and to draw the potential curves and vibrational energy levels in Fig. 1 are given in Table I.

The calculated kinetic energy distributions of Auger electrons for the $(1\sigma_u^{-1}1\pi_g^3) \rightarrow (1\pi_g^2)$ decay of the core-excited O_2 are shown in Figs. 2 and 3, for the radiation bandwidth broader ($\Gamma_L = 500$ meV), and narrower ($\Gamma_L = 50$ meV), respectively, than the actual lifetime width of the core-excited state ($\Gamma = 180$ meV). This lifetime width was used to calculate the spectra in the panels at the right sides of both figures; for comparison, spectra for a fictitious lifetime, five times longer than the actual one ($\Gamma = 36$ meV), are shown at the left sides. The independent variable is the relative kinetic energy of emitted Auger electrons, $\mathcal{E}^{\rm rel} = \mathcal{E} - (E^d_{v=0} - E^f_{n'=0'}) = \mathcal{E} - 518.5$ eV (if $E^d_{v=0} - E_{\rm in} = 530.2$ eV [6] and $E^f_{n'=0} - E_{\rm in} = 12.05$ eV [22]; these values chosen from the

TABLE I. Parameters used to construct the Morse potentials for V_g, V_d, and V_f [6].

	ω_e (cm^{-1})	$\omega_e x_e$ (cm^{-1})	r_e (Å)
$O_2(X^2\Sigma_g^-)$	1580.19	11.98	1.2074
$O_2^*(3\Pi_u)[1\sigma_u^{-1},1\pi_g^3]$	1097.18	14.023 [a]	1.3540
$O_2^+(X\ ^2\Pi_g)[1\pi_g]$	1904.77	16.26	1.1162

[a] $x_e\omega_e$ modified from 10.75 cm^{-1} to reproduce the dissociation energy $D_0 = 20\,915.35$ cm^{-1}.

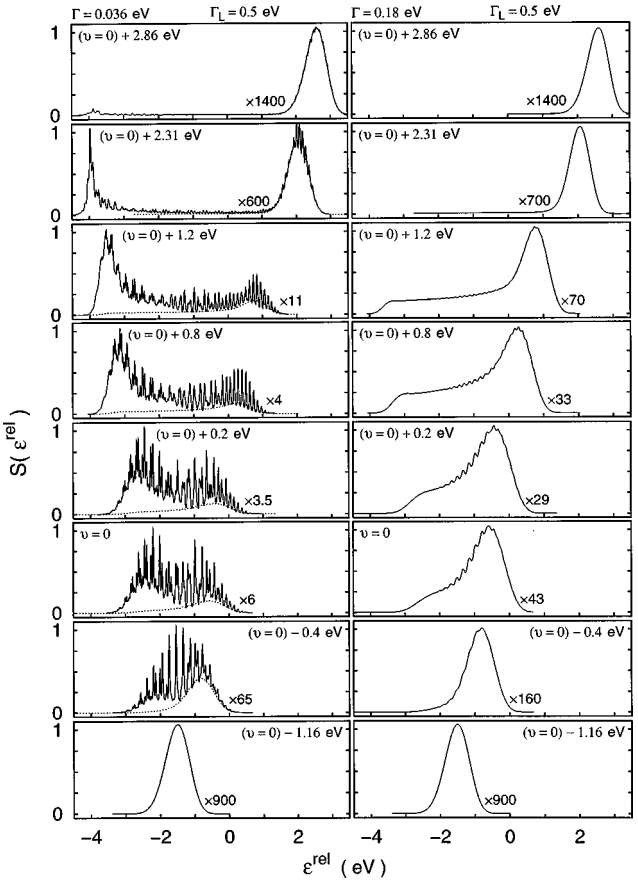

FIG. 2. Calculated decay electron spectra for the O_2 molecule for all x-ray excitations shown in Fig. 1 (the panel labels give the excitation energy with respect to the $v=0$ resonant excitation) for the x-ray bandwidth $\Gamma_L = 0.5$ eV, i.e., broader than the actual lifetime width of the core-excited state. The panels at right show the spectra for the actual lifetime width ($\Gamma = 0.18$ eV) and in the left panels hypothetical spectra for the five times smaller lifetime width are shown for comparison. The electron resolution is always assumed to be ideal. The spectra from the right panels are also reproduced by dotted lines in the left panels for comparison.

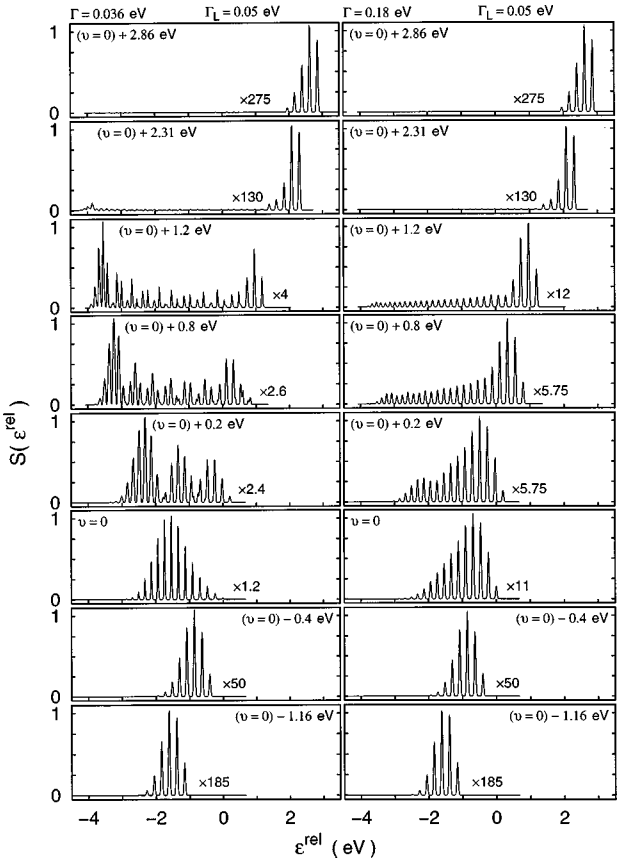

FIG. 3. The same as in Fig. 2 but for the x-ray bandwidth $\Gamma_L = 0.05$ eV, i.e., narrower than the actual lifetime width of the core-excited state.

literature do not affect the shapes of the calculated spectra). The panels in the horizontal rows correspond to eight different tuning conditions of the incident radiation which are specified by the *x-ray excitations* shown already in Fig. 1 and defined as $\hbar\omega_L^{\rm rel} = \hbar\omega_L - (E^d_{v=0} - E_{\rm in})$, i.e., $\hbar\omega_L^{\rm rel} = 0$ corresponds to radiation with $\hbar\omega_L = 530.2$ eV [6] tuned resonantly to the $v = 0$ vibrational level of V_d. The most efficient resonant excitation (to $v = 4$), i.e., $\Omega \approx 0$, corresponds to $\hbar\omega_L^{\rm rel} = +0.51$ eV. This means that extreme detuning conditions are met for the panels in the two horizontal rows at the top and the two at the bottom in Figs. 2 and 3, while the ones in the two central rows effectively correspond to little detuning.

The best insight into the properties of the spectra is gained by discussing their various features for Figs. 2 and 3 simultaneously. While experimental spectra exist [6,14] corresponding to the $\hbar\omega_L^{\rm rel} = -0.4, +0.2, +0.8$, and $+1.2$ eV panels at the right-hand side of Fig. 2, it is expected that spectra obtained with the x-ray bandwidths comparable to that in Fig. 3 should be available soon.

We start our discussion with the bottom panels in Fig. 2. For extreme detuning the spectrum consists of one essentially symmetric broad peak. More importantly, for both lifetimes the spectra are *identical*. Obviously, the wave-packet time evolution along the core-excited state surface does play a minimal role in the formation of the spectrum. The same effect is observed for large positive detunings: the spectra in the top horizontal row are again almost independent of the core-hole lifetime. The lifetime independence of the extremely detuned spectra is even more strikingly observed for the narrow excitation bandwidth in Fig. 3, where the detailed vibrational structure due to the final state (post Auger decay) ion is identical in the short and long lifetime spectra even for less extreme detuning than in Fig. 2. For such less extreme detunings, such as $\hbar\omega_L^{\rm rel} = -0.4$ eV, the broad excitation spectra in Fig. 2 depend on the lifetime quite strongly, because here a significant fraction of photons is present in the beam for which the detuning is rather small.

The lifetime independence of the spectra does not necessarily mean that the spectrum is not affected by the time evolution in the core-excited state, but merely that the effective relevant time evolution determined by $\Gamma_{\rm eff}$ in Eq. (2) is much shorter than the actual (and the hypothetically lengthened) lifetime. For example, the relative heights of the final-state vibrational peaks in the panels for less extreme detuning ($\hbar\omega_L^{\rm rel} = -0.4$ eV and $+2.31$ eV) in Fig. 3 are different from their more extremely detuned counterparts (-1.16 eV and $+2.86$ eV, respectively). In the case of a truly evolution-independent situation, these spectra would be identical apart from a rigid displacement along the electron kinetic energy axis due to energy conservation. Even the spectra for the most extreme detuning are visibly affected by the time evolution, but only in the narrow excitation bandwidth case in Fig. 3, where the relative heights of the peaks are somewhat different in the spectra for $\hbar\omega_L^{\rm rel} = -1.16$ eV from those in the $+2.86$ eV spectra. This difference is lost for the broad excitation case in Fig. 2: apart from the shift, the spectra in the bottom panels are virtually identical to the spectra at the top.

As the detuning decreases, the spectra become more complicated, and their appearance strongly depends on the lifetime. Ignoring details, we see that for higher excitation energies the spectra are generally broader, and for a longer lifetime more slow electrons than fast ones are emitted. Taking the left-hand side $\hbar\omega_L^{\rm rel} = +1.2$ eV panel in Fig. 2 as an example, we see that the emitted electrons may be grouped into a majority of slow ones and a minority of fast ones, their kinetic energies differing by some 4.5 eV, with almost no electrons with intermediate kinetic energies. This is a classical effect already shown in Fig. 1: if we project the classical turning points in V_d, which correspond to the $+1.2$ eV excitation, down onto V_f, we get the classical turning points of the latter separated by an energy of about 4.5 eV. Classically, the molecule in the core-excited state is more likely to decay near one of its classical turning points than anywhere in between, if only the lifetime is long enough to allow the molecule to visit both of them repeatedly. This is, of course, the case for the long lifetime chosen in the left side panels. The above argument works even more beautifully for very large positive detuning of $+2.31$ eV. Going down with the excitation energy, the low- and the high-energy groups get closer to each other (as expected from the above classical picture) and start to overlap. For the actual short lifetime (right panels in Fig. 2) the molecules do not have much chance to perform even one oscillation before the decay takes place, so the majority of emitted electrons have relatively high kinetic energy with an extended low-energy tail

due to those molecules which, against the odds, have been able to survive long enough to get close to the outer turning point of V_d. To contrast the short and the long lifetime spectra, we have inserted in the left panels of Fig. 2, in dotted lines, the curves from the right panels preserving now their relative magnitudes. Ignoring vibrational structure details, the gross features of the high-energy part of the spectra are independent of the lifetime, while they are very different at the low-energy side. The buildup of the low-energy tail seen in the right panels of Fig. 2 as $\hbar\omega_L$ progresses from -0.4 through $+0.2$ and $+0.8$ to $+1.2$ was indeed recently observed and explained using arguments similar to ours [6,14]. The gradual increase of the low-energy fraction of emitted electrons was demonstrated in the recent explicitly time-dependent approach to ARRE [20] in which the formation of the spectra over femtosecond time scales (experimentally inaccessible) was followed by numerically solving the appropriate set of coupled Schrödinger equations.

The same general arguments can be used to interpret the gross features of the narrow excitation band spectra in Fig. 3. On its top, the spectra for the actual lifetime (right panels) contain detailed information about the vibrational structure of the final-state potential V_f. The central panels, corresponding to little or no detuning, exhibit a long tail of low energy peaks formed by electrons emitted by molecules which have survived for a relatively long time in the core-excited state. For the hypothetically prolonged lifetime, the low-energy peaks dominate the spectra. The double-peak structures observed for some lines in the central left-hand panels of Fig. 3 are a feature often observed under ARRE conditions [2,3]. The variations in the peak heights, the low-energy tail, etc., have encoded in them information about the core-excited state potential and about the core-hole lifetime. Certainly, this type of information is not easy to extract for a system for which no other independent information is available.

In conclusion, we have applied a recently developed time-dependent approach to investigate the decay electron spectra for O_2 molecules for excitation bandwidths above and below the lifetime width of the core-excited state. A fictitious long lifetime has also been used to emphasize interpretational aspects of the influence on the spectra due to the detuning of the incoming radiation away from the excitation resonances. The detuning behavior of the O_2 ARRE spectra distinctly differs from that for N_2 and CO [18], because for O_2 the intermediate state potential, V_d, is softer and has a larger internuclear equilibrium separation relative to both the initial- and the final-state potentials, V_g and V_f, respectively, than is the case for the other two molecules. Consequently, in contrast to N_2 or CO, certain gross features of the O_2 ARRE spectra can be understood in terms of the classical evolution of the system in the core-excited state (e.g., in terms of its classical turning points); the understanding of others, as well as of all details, requires the full quantum treatment.

We thank Wilfried Wurth for helpful discussions and for providing many experimental and interpretational insights. We are grateful to A.M. Bradshaw for preprints of Refs. [13,15] prior to acceptance. Z.W.G. would like to thank his colleagues at the Physik- Department of the Technical University of Munich for their hospitality during his visits there, and J.-P. de Villiers for writing the numerical code for the wave-packet propagation. This work has been supported by a research grant from the Natural Sciences and Engineering Research Council (NSERC) of Canada, and by SFB 338 of the Deutsche Forschungsgemeinschaft.

[1] *Resonant Anomalous X-ray Scattering: Theory and Applications*, edited by G. Materlik, C. Sparks, and K. Fisher (North-Holland, Amsterdam, 1994); in particular, see T. Åberg and B. Craseman, *ibid.*, p. 431 and references therein; P. L. Cowan, *ibid.*, p. 449.

[2] F. Gelmukhanov and H. Ågren, Phys. Lett. A **193**, 375 (1994).

[3] G. B. Armen and H. Wang, Phys. Rev. A **51**, 1241 (1995).

[4] E. Kukk, S. Aksela, and H. Aksela, Phys. Rev. A **53**, 3271 (1996).

[5] T. D. Thomas and T. X. Caroli, Chem. Phys. Lett. **185**, 31 (1991).

[6] M. Neeb, J.-E. Rubensson, M. Biermann, W. Eberhardt, K. J. Randall, J. Feldhaus, A. L. D. Kilcoyne, A. M. Bradshaw, Z. Xu, P. D. Johnson, and Y. Ma, Chem. Phys. Lett. **212**, 205 (1993).

[7] S. J. Osborne, A. Ausmees, S. Svensson, A. Kivimäki, O. -P. Sairanen, A. Naves de Brito, H. Aksela, and S. Aksela, J. Chem. Phys. **102**, 7317 (1995).

[8] P. Skytt, P. Glans, K. Gunnelin, J. Guo, and J. Nordgren, Phys. Rev. A **55**, 146 (1997).

[9] M. N. Piancastelli, M. Neeb, A. Kivimäki, B. Kempgens, H. M. Köppe, K. Maier, and A. M. Bradshaw, Phys. Rev. Lett. **77**, 4302 (1996).

[10] S. Sundin, F. Kh. Gel'mukhanov, H. Ågren, S. J. Osborne, A. Kikas, O. Björnholm, A. Ausmees, and S. Svensson, Phys. Rev. Lett. **79**, 1451 (1997).

[11] M. N. Piancastelli, M. Neeb, A. Kivimäki, B. Kempgens, H. M. Köppe, K. Maier, A. M. Bradshaw, and R. F. Fink, J. Phys. B **30**, 5677 (1997).

[12] C. Keller, M. Stichler, G. Comelli, F. Esch, S. Lizzit, W. Wurth, and D. Menzel, Phys. Rev. Lett. **80**, 1774 (1998); C. Keller, M. Stichler, G. Comelli, F. Esch, S. Lizzit, D. Menzel, and W. Wurth, J. Electron Spectrosc. Relat. Phenom. **93**, 135 (1998).

[13] M. N. Piancastelli, A. Kivimäki, B. Kempgens, M. Neeb, K. Maier, U. Hergenhahn, A. Rüdel, and A. M. Bradshaw, J. Electron Spectrosc. Relat. Phenom. (to be published).

[14] M. Neeb, J.-E. Rubensson, M. Biermann, and W. Eberhardt, J. Electron Spectrosc. Relat. Phenom. **67**, 261 (1994).

[15] A. Kivimäki, B. Kempgens, M. N. Piancastelli, M. Neeb, K. Maier, A. Rüdel, U. Hergenhahn, and A. M. Bradshaw, J. Electron. Spectrosc. Relat. Phenom. **93**, 81 (1998).

[16] E. Kukk, H. Aksela, S. Aksela, F. Gel'mukhanov, H. Ågren, and S. Svensson, Phys. Rev. Lett. **76**, 3100 (1996).

[17] O. Björneholm, S. Sundin, S. Svensson, R. R. T. Marinho, A. Naves de Brito, F. Gel'mukhanov, and H. Ågren, Phys. Rev. Lett. **79**, 3150 (1997).

[18] Z. W. Gortel, R. Teshima, and D. Menzel, Phys. Rev. A **58**, 1225 (1998).
[19] L. S. Cederbaum and F. Tarantelli, J. Chem. Phys. **98**, 9691 (1993).
[20] E. Pahl, H.-D. Meyer, and L. S. Cederbaum, Z. Phys. D **38**, 215 (1996).
[21] F. Gelmukhanov, T. Privalov, and H. Ågren, Zh. Eksp. Teor. Fiz. **112**, 37 (1997) [JETP **85**, 20 (1997)]; Phys. Rev. A **56**, 256 (1997).
[22] P. H. Krupienie, J. Phys. Chem. Ref. Data **1**, 423 (1972).